Large basis space effects in electron scattering form factors of light nuclei

K. Amos and C. Steward
School of Physics, The University of Melbourne, Parkville, Victoria 3052, Australia
(Received 15 May 1989)

Large basis space projected Hartree-Fock wave functions have been used to calculate the longitudinal and transverse (electric) form factors from the excitations of 2_1^+ and 4_1^+ states in ^{12}C, ^{20}Ne, and ^{24}Mg. The results obtained by use of such large basis space models of structure are compared with limited basis space (shell-model) predictions to show that momentum-transfer-dependent corrections can be quite diverse.

I. INTRODUCTION

Transition density-matrix elements for excitation of the low-lying isoscalar 2^+ and 4^+ states in ^{20}Ne and ^{24}Mg have been defined from both small basis [*s-d* shell; SU(3)] and large basis projected Hartree-Fock (PHF) models of nuclear spectroscopy[1,2] and then used to analyze both electromagnetic and hadron inelastic scattering data. The former specifically were $B(CL)$ values and electron scattering longitudinal form factors while the latter included polarizations and analyzing powers from inelastic proton scattering. From such analyses[2] of complementary data, consistent values for effective charges for each (small basis) model were determined. Further, comparisons of the results calculated using transition density-matrix elements from both small and large basis structure models showed that those effective charges primarily reflect $2\hbar\omega$ excitations out of the $0p$ and $1s$-$0d$ shells. Those conclusions have not changed despite many subsequent studies of properties of the *s-d* shell nuclei. Indeed from a recent review[10] of the status of the shell model it was concluded "that non-*s-d* shell contributions (to form factors) must be included at a more explicit level than as effective operators, in ways that are as yet not understood." Hence use of the large basis space PHF models remains as a most convenient way to study, in select transitions, the effects of mixing of $2\hbar\omega$ and higher excitations in low-lying spectra; a study that Brown and Wildenthal[10] ascribe as "another challenge for the future."

Of particular concern regarding $2\hbar\omega$ excitations out of the $0p$ and $0d$-$1s$ shells is that there could be significant momentum-transfer dependencies in form factors to make them quite different from those obtained using simple (valence) shell models. In this context, the analyses[2] of the electron scattering longitudinal form factors data are of particular interest to recall since, recently, transverse form factor data form ^{24}Mg have been measured.[3] Such data are additional and rather more stringent tests of the models of spectroscopy. Also, as evident from Fig. 1 of Ref. 2, the longitudinal form factor data from, and the calculated result for, the 4_1^+ (4.12 MeV) state in ^{24}Mg are quite different functions of momentum transfer from those for excitation of the 4_1^+ states in ^{20}Ne and ^{28}Si.

II. NOMENCLATURE AND CALCULATION DETAILS

For light nuclei, electron scattering form factors can be calculated with confidence in a plane-wave approximation when corrections are made for center-of-mass motion and finite nucleon size.[4] Then form factors for angular momentum transfer I and three-momentum transfer q can be expressed as

$$|F_\eta^{(I)}(q)|^2=(4\pi/Z^2)f_{\rm rec}|\langle\psi_{J_f}\|Q_\eta^{(I)}(q)\|\psi_{J_i}\rangle|^2/(2J_i+1)\ , \tag{1}$$

in which η designates longitudinal (L) or transverse (T), and $f_{\rm rec}$ is an appropriate recoil and particle size factor. The reduced matrix elements may be expressed in terms of spectroscopic amplitudes per

$$\langle\psi_{J_f}\|Q_\eta^{(I)}(q)\|\Psi_{J_i}\rangle=\mathrm{Tr}(SM)/(2I+1)^{1/2}\ , \tag{2}$$

in which the single-particle expectation values

$$M_{j_1j_2I}^{(\alpha)}=\langle\phi_{j_2}^{(\alpha)}\|Q_\eta^{(I)}(q)\|\phi_{j_1}^{(\alpha)}\rangle \tag{3}$$

are standard[4] with α designating proton ($\alpha=-\frac{1}{2}$) and neutron ($\alpha=\frac{1}{2}$), and the spectroscopic amplitudes are as defined previously,[1,2]

$$S_{j_1j_2I}^{(\alpha)}=\langle\psi_{J_f}\|[a_{j_2}^\dagger\times a_{j_1}]_{(\alpha)}^I\|\psi_{J_i}\rangle\ . \tag{4}$$

These spectroscopic amplitudes are the reduced one-body density-matrix elements for excitation of the residual nuclear state (ψ_{J_f}) by changing a nucleon of type α from shell j_1 to shell j_2. As we will be concerned with extensive (large basis) tables of such amplitudes, it is convenient to use a single-particle hierarchy as given in Table I. Hereafter in tables and figures, select components will be identified by either the specific orbit *ID* or the relevant oscillator unit, N, given therein.

We have investigated properties of (longitudinal and transverse) form factors from excitation of the 2_1^+ (4.44 MeV) state in ^{12}C, of the 2_1^+ (1.63 MeV) and 4_1^+ (4.25 MeV) states in ^{20}Ne, and of the 2_1^+ (1.37 MeV), 2_2^+ (4.23 MeV), and 4_1^+ (4.17 MeV) states in ^{24}Mg. With the ex-

TABLE I. Single-particle orbit hierarchy and identification. The oscillator unit N is given by $2n+1$ for any orbit.

$N=0$		$N=1$		$N=2$		$N=3$		$N=4$	
ID	Orbit	*ID*	Orbit	*ID*	Orbit	*ID*	Orbit	*ID*	Orbit
1	$0s_{1/2}$	2	$0p_{3/2}$	4	$0d_{5/2}$	7	$0f_{7/2}$	11	$0g_{9/2}$
		3	$0p_{1/2}$	5	$0d_{3/2}$	8	$0f_{5/2}$	12	$0g_{7/2}$
				6	$1s_{1/2}$	9	$1p_{3/2}$	13	$1d_{5/2}$
						10	$1p_{1/2}$	14	$1d_{3/2}$
								15	$2s_{1/2}$

ception of the 2_2^+ excitation in ^{24}Mg, large basis space projected Hartree-Fock calculations have given extensive sets of spectroscopic amplitudes for these transitions. The complete sets for the transitions in neon have been published,[1] but only limited lists have been given for the others.[1,2] The limitations, which were made for convenience and were based upon the size of the amplitudes, had little effect upon calculations of either the $B(CL)$ values or the longitudinal form factors. Such is not necessarily the case for the transverse form factors, and so we give a full list of amplitudes for the ^{12}C 2_1^+ excitation in Table II, for the ^{24}Mg 2_1^+ excitation in Table III, and for the ^{24}Mg 4_1^+ excitation in Table IV.

In Table II, the spectroscopic amplitudes of the 2_1^+ excitation in ^{12}C were obtained from a PHF calculation made using energies and potentials of Bassichis *et al.*[5] and the set is designated as PHF BA. They have been scaled by a factor of 10^3 and grouped in three parts. The first part is identified as the $0p$ shell contributions; the values in which are quite similar to those obtained by the standard ($0p$) shell-model calculations of Cohen and Kurath.[6] The second set form the group defined as set 1, and these values together with the $0p$-shell contributions were tabled and used previously.[1] The remainder from the complete PHF calculations are defined as set 2.

TABLE II. The PHFBA spectroscopic amplitudes ($S_{J_1J_2^2}\times 10^3$) for the excitation of the 2_1^+ (4.44 MeV) state in ^{12}C.

$0p$ shell		Set 1		Set 2	
$j_1{:}j_2$	S	$j_1{:}j_2$	S	$j_1{:}j_2$	S
2:2	549.2	1:4	−234.2	2:9	9.0
2:3	−1086.0	1:5	208.7	2:10	−10.5
3:2	804.2	2:7	−197.3	4:4	−9.9
		2:8	88.0	4:5	5.4
		3:8	−56.2	4:6	−7.1
		3:9	42.8	5:4	−5.4
		4:1	−127.8	5:5	−9.0
		5:1	−114.1	5:6	−6.3
		7:2	−64.0	6:4	−12.9
		8:3	−44.6	6:5	11.5
		9:2	−53.6	7:7	−4.0
				7:8	1.5
				7:9	−2.9
				8:7	−2.4
				8:8	−0.6
				8:9	−1.7
				8:10	−2.9
				9:2	15.1
				9:7	−8.9
				9:8	3.3
				9:10	−0.5
				10:2	7.8
				10:8	−0.5
				10:9	0.4

The transition densities for ^{24}Mg (2_1^+ and 4_1^+) were obtained from the Hartree-Fock calculations of Ford *et al.*,[7] and the spectroscopic amplitudes for the 2_1^+ excitation are listed in Table III. Again the $1s$-$0d$ shell components are very similar to those generated using a standard (s-d) shell model.[1] Together with the set 1 values they were used previously[1,2] in analyses of (longitudinal) form factor data. The missing values (set 2) in this case are numerous and have been grouped in terms of the parity of the single-nucleon orbits involved.

The 4_1^+ excitation in ^{24}Mg, when specified by the same projected Hartree-Fock method,[7] gives the spectroscopic amplitudes that are listed in Table IV and which are grouped according to the hierarchy of oscillator units. The first entry of Table IV, designated as $2\rightarrow 2$, gives the $1s$-$0d$ shell values. They are very like the values determined from standard (s-d) shell-model studies.

All of the calculated results reported herein were made using harmonic-oscillator wave functions. For ^{12}C an oscillator length of 1.7 fm was used while a value of 1.9 fm was chosen for the calculations involving ^{20}Ne and ^{24}Mg. With those values, previous calculations[1,2] of $B(CL)$ and longitudinal form factors[1,2] were in good agreement with data. But the transverse form factors are more sensitive to details, and we note the effects found recently[8] when Woods-Saxon rather than harmonic-oscillator wave functions were used. With our large basis space calculations, however, we are uncertain as to what finite well to use to define $N=3$ and 4. However, to a certain extent the large basis Hartree-Fock calculation equates to improving single-particle wave functions from the initial (harmonic-oscillator) ones.

III. RESULTS AND DISCUSSION

The form factors from excitation of the 2_1^+ states in ^{12}C (4.44 MeV), ^{20}Ne (1.63 MeV), and ^{24}Mg (1.37 MeV) and as calculated using the PHF models of structure are shown in Fig. 1; the longitudinal ones on the left and transverse ones on the right. The short-dash lines depict

TABLE III. The PHF spectroscopic amplitudes ($S_{j_1 j_2 2} \times 10^3$) for the excitation of the 2_1^+ (1.37 MeV) state in ^{24}Mg.

				Set 2			
1s-0d shell		Set 1		positive parity		negative parity	
j_1:j_2	S	j_1:j_2	S	j_1:j_2	S	j_1:j_2	S
4:4	831	1:4	−164	1:6	50	2:2	16
4:5	−574	1:5	123	4:12	76	2:3	−13
4:6	681	2:7	−227	4:14	52	2:9	−37
5:4	595	2:8	105	5:13	98	2:10	30
5:5	−15	3:8	−217	5:15	44	3:2	13
5:6	197	4:1	−209	11:11	10	3:9	−38
6:4	543	4:11	−192	11:13	20	7:7	13
6:5	−232	4:13	142	12:4	−53	7:8	−5
		4:15	153	12:5	−28	8:2	−82
		5:1	−103	12:11	5	8:7	5
		5:12	−40	12:13	−9	8:8	16
		6:13	84	13:1	−61	8:9	−22
		6:14	−13	13:12	13	8:10	−37
		7:2	−176	13:13	24	9:2	−27
		7:9	−46	13:14	−9	9:3	28
		8:3	−168	13:15	24	9:8	28
		9:7	−60	14:1	−39	9:9	−18
		10:8	−48	14:4	54	9:10	15
		11:4	−120	14:6	11	10:2	−22
		13:4	140	14:13	9	10:9	−14
		13:6	108	15:5	−51		
		13:11	−32	15:13	18		
		15:4	122				

TABLE IV. The PHF spectroscopic amplitudes ($S_{j_1 j_2 4} \times 10^3$) for the excitation of the 4_1^+ (4.12 MeV) state in ^{24}Mg. The amplitudes are grouped according to the single-particle orbit hierarchy with those labeled *E* being additional to the set given in Ref. 2.

$\hbar\omega$ units	j_1:j_2	S	j_1:j_2	S	j_1:j_2	S
2→2	4:4	−784.9	4:5	−347.2	5:4	118.1
3→3	7:7	10.1	8:8	11.5	8:9	10.3
	9:8	−15.0				
E	7:8	−7.2	7:9	3.6	7:10	−5.5
E	8:7	7.1	9:7	2.9	10:7	14.2
4→4	11:15	−18.9	12:13	−14.5	12:15	−7.9
	13:11	−13.8	13:12	21.6	13:13	−18.2
	15:11	−22.2	15:12	15.2		
E	11:11	8.9	11:12	−8.2	11:13	−10.2
E	11:14	5.6	12:11	9.3	12:12	0.5
E	12:14	0.7	13:14	−8.0	14:11	−9.0
E	14:12	1.9	14:13	3.9		
1→3	2:7	−50.3	2:8	−30.2	3:7	14.2
3→1 *E*	7:2	−2.8	7:3	−5.4	8:2	−11.8
2→4	4:11	−80.6	4:12	130.1	4:13	−118.0
	4:14	−41.0	5:11	−100.4	5:12	24.4
	5:13	24.9	6:11	−98.6	6:12	51.2
4→2	11:4	−57.3	11:5	60.8	1:6	−84.0
	12:4	−87.9	12:5	11.7	12:6	−34.7
	13:4	−124.5	13:5	−61.6	14:4	15.4
0→4	1:11	22.2	1:12	−12.9		
4→0	11:1	22.3	12:1	−10.1		

the results obtained when only the valence shell (0*p* for ^{12}C and 1*s*-0*d* for ^{20}Ne, ^{24}Mg) spectroscopic amplitudes are used. Those results are essentially what one would obtain with any standard (0*p* or 1*s*-0*d* basis) shell model of spectroscopy. The long-dash lines depict the results obtained when the published,[1,2] limited (by size) set of PHF spectroscopic amplitudes were used. The complete set of PHF amplitudes given in Tables II and III were used to obtain the results depicted by the continuous lines.

Clearly the full PHF longitudinal form factors, which fit the data to 2 fm^{-1}, are well approximated by the calculations made using the limited set of spectroscopic amplitudes. So also do the valence shell-model calculations (to 1.5 fm^{-1}) when appropriate effective charges are used. But the transverse form factors are much more sensitive to the specific set of spectroscopic amplitudes, and quite clearly, the valence shell-model results are different from those calculated using the complete PHF spectroscopic amplitude set, and in the 0 to 2 fm^{-1} range in particular. Furthermore, the (many) small spectroscopic amplitudes that could reasonably be ignored in analyses of the longitudinal data are of some significance in calculations of the transverse form factor. Those small amplitude effects are more serious for ^{24}Mg than for ^{12}C.

The longitudinal and transverse form factors for excitation of the 4_1^+ (4.25 MeV) state in ^{20}Ne and of the 4_1^+ (4.12 MeV) state in ^{24}Mg are displayed in the left and right panels of Fig. 2, respectively. Therein the results obtained using the complete PHF model spectroscopic amplitudes are displayed by the continuous curves. When the limited (by size) PHF spectroscopic amplitudes were used the results depicted by the long-dash curves were obtained while the short-dash curves depict results obtained using the *s-d* parts of the PHF model. It is evident that the 4_1^+ longitudinal form factors for ^{20}Ne are related simply by an effective charge, but that is not the case for ^{24}Mg. Use of large basis space spectroscopy (limited or not) for the ^{24}Mg 4_1^+ excitation changes the longitudinal form factor from that of any (standard) *s-d* shell model, in shape as well as in magnitude. This point was observed previously,[2] and more specifics will be discussed in the following in connection with Fig. 3. The *s-d* and complete PHF models give transverse form factors for ^{20}Ne that also are distinctively different; albeit not as dramatically different at the relevant 2_1^+ transverse form factors shown in Fig. 1. On the other hand, the calculat-

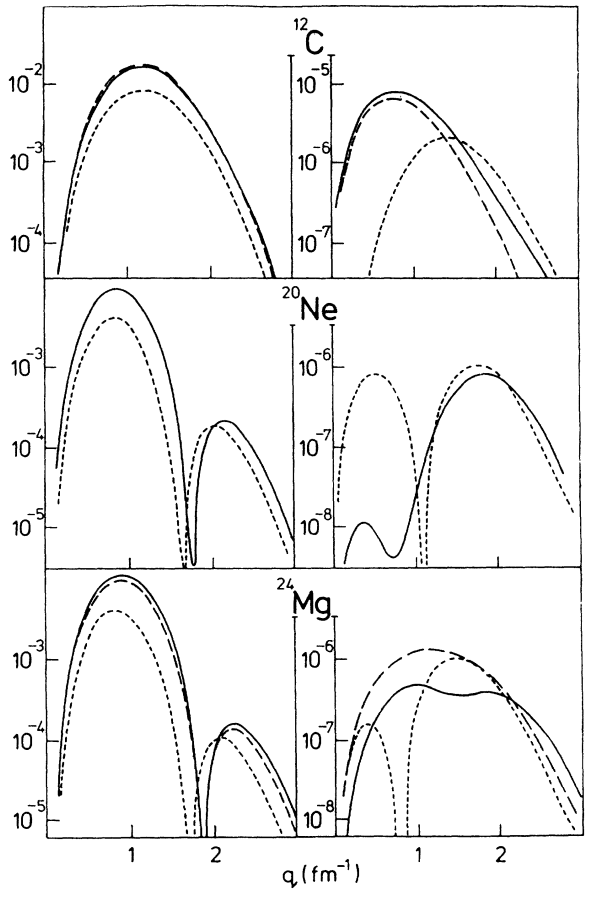

FIG. 1. The form factors for the excitation of the 2_1^+ states in ^{12}C (4.44 MeV), ^{20}Ne (1.63 MeV), and ^{24}Mg (1.37 MeV); the longitudinal ones on the left and transverse ones on the right. The short-dash lines depict the results obtained using only valence shell spectroscopic amplitudes in calculations while the long-dash lines were obtained using the restricted set of PHF spectroscopic amplitudes. The results of calculations made using the complete PHF sets of amplitudes are depicted by the continuous lines.

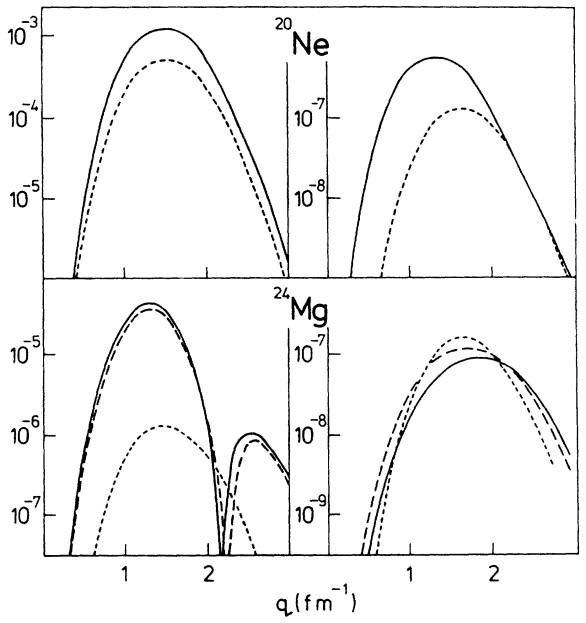

FIG. 2. The longitudinal and transverse form factors for excitation of the 4_1^+ (4.25 MeV) state in ^{20}Ne and of the 4_1^+ (4.12 MeV) state in ^{24}Mg are displayed in the left and right panels, respectively. The short-dash curves depict the results obtained using the *s-d* valence shell spectroscopic amplitudes of the PHF models, the long-dash curves display results obtained using the complete limited (by size) PHF model, and the results of using the complete PHF models are depicted by the continuous lines.

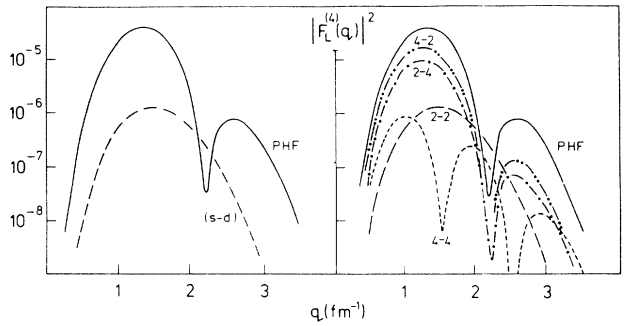

FIG. 3. Longitudinal form factors for the 4_1^+ (4.12 MeV) state in ^{24}Mg. In both panels the continuous curve depicts the complete PHF model result. On the right, the component parts of the full PHF result are shown, with the corresponding labels denoting the initial-final shells of the nucleons contributions, according to the convention in Tables I and IV. The 2-2 curve is therefore identical to that identified as *s-d* in the left panel.

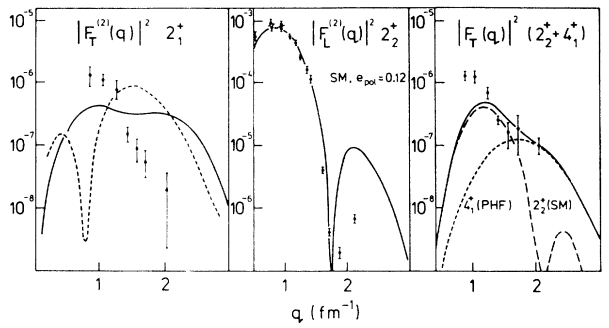

FIG. 4. The transverse 2_1^+, longitudinal 2_2^+, and the summed, transverse $(2_2^+ + 4_1^+)$ form factors for ^{24}Mg. The curves labeled SM depict the (*s-d*) shell-model result while those labeled PHF denote the complete PHF result. The experimental data in the left and right panels is from Ref. 3 while that of the center panel is from Ref. 2.

ed transverse form factors for the 4_1^+ excitation in ^{24}Mg are remarkably similar, and it is the longitudinal form factor for this transition that is of most interest. Thus the component contributions to this longitudinal form factor are displayed in Fig. 3. In both panels the continuous curve depicts the complete PHF model result, and is so labeled. With the unusual minimum at 2.1 fm^{-1} this gave a reasonable fit to the measured data,[9] which the *s-d* shell result, even scaled by an effective charge, cannot. The component parts are shown in the right-hand panel with the labels denoting the initial-final shells of the active nucleons in the calculations. The 2-2 curve is therefore that labeled as (*s-d*) on the left, and so the distinctive shape of the full PHF model result is due to $2\hbar\omega$ excitations between the (*s-d*) $N=2$ and (*g-s-d*) $N=4$ levels. The negative-parity contributions (1–3, etc.) are quite small and so are not shown. With the $N=4$ shell incorporating the 1*d* and 2*s* orbits, contributions in which they link with the 0*d* and 1*s* orbits, respectively, may be evidence of single-particle wave functions being different from the harmonic oscillators that we have used, as is suggested from a recent study of ^{13}C data.[8] However, only the ^{24}Mg longitudinal form factor is distinctively altered when large basis space functions are used. The harmonic-oscillator models fit the longitudinal data from ^{20}Ne and ^{28}Si very well.[1,2]

Transverse form factor data from ^{24}Mg have been measured recently.[3] In that experiment, the 2_1^+ state data were resolved, but the 4_1^+ values could not be isolated from the 2_2^+ state (4.23 MeV) contributions. To compare our calculated results with these data therefore, we need to estimate the 2_2^+ state contributions. We do not have a satisfactory large basis model of structure for this state, but fortunately, the standard *s-d* shell model with a polarization charge of only 0.12*e* gives an excellent fit to the longitudinal form factor (to 1.8 fm^{-1}). Hopefully the same model spectroscopy gives a reasonable estimate of the transverse form factor for the 2_2^+ state. We assume so, and the results are presented in Fig. 4. From left to right in this figure are displayed the transverse 2_1^+, the longitudinal 2_2^+, and the summed, transverse $(2_2^+ + 4_1^+)$ form factors for ^{24}Mg. It is rather disappointing to observe the mismatch between the full PHF model calculated result and the 2_1^+ transverse form factor data.[3] The changes wrought by using the large basis space model of structure, unlike those which occurred in a study[1] of the equivalent ^{12}C form factor, do not give even the trend of observation.

The longitudinal form factor for the 2_2^+ state excitation[2] is reproduced herein as it is the justification for use of a shell model to estimate the transverse form factor that is shown in the far right panel of Fig. 4. Under the circumstances our calculated results seem reasonable. But clearly we would like more data with better resolution, and at smaller momentum-transfer values. Such data from the other $N=Z$ *s-d* shell nuclei would also be useful.

IV. CONCLUSIONS

This study of longitudinal and transverse form factors from excitation of 2_1^+ and 4_1^+ states in select light nuclei has shown that using large basis space models of nuclear structure can drastically alter predictions of electron scattering form factors from those given by small basis models of structure. While that is particularly the case with the transverse form factors, such may also occur with the longitudinal form factors.

By and large, our calculations made using large basis PHF wave functions and with the valence shell [0*p* for ^{12}C, (0*d*-1*s*) for ^{20}Ne and ^{24}Mg] have very similar shapes. For $q < 1.5$ fm^{-1} they usually relate by a simple scaling, thereby defining an effective charge. But the longitudinal form factors from calculation of the 4_1^+ excitation in ^{24}Mg have no such simple relationship. In this case, large basis structure results in a new momentum transfer

dependence in predictions and one that is confirmed by data.

But it is in the calculated results for transverse form factors that large basis effects are very evident. In all cases the complete PHF model results differ noticeably as functions of q from those obtained using just the relevant valence space (shell-model) spectroscopic amplitudes. We have also seen that numerous small magnitude amplitudes cannot be ignored in such calculations but that on the basis of the present data, the current large basis PHF model is still not a satisfactory representation of details of (microscopic) structure.

[1]P. Nesci and K. Amos, Nucl. Phys. **A284**, 239 (1977); K. Amos, P. Nesci, and I. Morrison, Aust. J. Phys. **33**, 495 (1980); K. W. Schmid, Phys. Rev. C **24**, 1283 (1981); K. Amos and I. Morrison, Phys. Rev. C **19**, 2108 (1979).

[2]K. Amos and W. Bauhoff, Nucl. Phys. **A424**, 60 (1984).

[3]A. Hotta, R. S. Hicks, R. L. Huffman, G. A. Peterson, R. J. Peterson, and J. R. Shepard, Phys. Rev. C **36**, 2212 (1987).

[4]T. Donnelly and J. D. Walecka, Annu. Rev. Nucl. Sci. **25**, 329 (1975); T. de Forest and J. D. Walecka, Adv. Phys. **15**, 1 (1966); H. Uberall, in *Electron Scattering from Complex Nuclei,* Vol. 36 of *Pure and Applied Physics,* edited by H.S.W. Massey and K. A. Brueckner (Academic, New York, 1971).

[5]W. H. Bassichis, A. K. Kerman, and J. P. Svenne, Phys. Rev. **160**, 746 (1967).

[6]S. Cohen and D. Kurath, Nucl. Phys. **73**, 1 (1965).

[7]W. C. Ford, R. C. Braley, and J. Bar-Touv, Phys. Rev. C **4**, 2099 (1971).

[8]D. J. Millener, D. I. Sober, H. Crannell, J. T. O'Brien, L. W. Fagg, S. Kowalski, C. F. Williamson, and L. Lapikas, Phys. Rev. C **39**, 14 (1989).

[9]H. Zarek, S. Yen, B. O. Pich, T. E. Drake, C. F. Williamson, S. Kowalski, C. P. Sargent, W. Chung, B. H. Wildenthal, M. Harvey, and H. C. Lee, Phys. Lett. **80B**, 26 (1978).

[10]B. A. Brown and B. H. Wildenthal, Annu. Rev. Nucl. Part. Sci. **38**, 29 (1988).